PHASE PORTRAITS OF (2;0) REVERSIBLE VECTOR FIELDS WITH SYMMETRICAL SINGULARITIES

CLAUDIO BUZZI[1], JAUME LLIBRE[2] AND PAULO SANTANA[3]

Abstract. In this paper we study the phase portraits in the Poincaré disk of the reversible vector fields of type (2;0) having generic bifurcations around a symmetric singular point p. We also prove the nonexistence of any periodic orbit surrounding p. We point out that some numerical computations were necessary in order to control the number of limit cycles.

1. Introduction and Main Results

Given two real C^k, $k \geqslant 1$, functions of two variables P, $Q : \mathbb{R}^2 \to \mathbb{R}$ we define a *planar C^k differential system* as a system of the form

$$\dot{x} = P(x, y), \qquad \dot{y} = Q(x, y), \tag{1}$$

where the dot in system (1) denotes the derivative with respect to the independent variable t. We call the map $X = (P, Q)$ a *vector field*. If P and Q are polynomials then system (1) is a *planar polynomial differential system*. In this case we say that system (1) has *degree* n if the maximum of the degrees of P and Q is n. If $n = 1$ then system (1) is called a *linear differential system*. This last class of systems is already completely understood (see for instance chapter 1 of [17]). However for $n \geq 2$, that is for nonlinear differential polynomial systems we know very few things. The class of planar polynomial systems with degree $n \geq 2$ is too wide, so is common to study more specific subclasses and to classify their topological phase portraits. See for instance [1], [10] and [23].

In this paper we are concerned with the *reversible vector fields*. Given a C^k vector field X (not necessarily planar) and a C^k diffeomorphism $\varphi : \mathbb{R}^m \to \mathbb{R}^m$ satisfying $\varphi^2 = id_{\mathbb{R}^m}$ we say that X is φ-reversible of type $(m; r)$, for $r \in \{0, 1, \ldots, m\}$, if

$$D\varphi(z)X(z) = -X(\varphi(z))$$

for all $z \in \mathbb{R}^m$ and $Fix(\varphi) = \{z \in \mathbb{R}^m : \varphi(z) = z\}$ is a r-dimensional manifold. Many types of reversible vector fields have been studied for several

2010 *Mathematics Subject Classification.* Primary 34C05, 34C14.

Key words and phrases. Reversibility, phase portrait, reversible vector fields, classification of vector fields, Poincaré disk.

authors. For example in [22] all the low codimension singularities of systems (2;1)-type are classified, in [4] all (3;2)-type. In [15, 16] there is a study of the quadratic reversible vector fields of type (3;2) on the sphere $\mathbb{S}^2$.

In the space of planar C^∞ reversible vector fields we consider the following equivalence relation: $X \sim Y$ if there is a neighborhood U of $(0,0)$ such that X and Y coincide in U. The equivalence class of X is called the *germ* of X. We will denote the germ of X also by X. In this paper we study the space of germs of C^∞ reversible vector fields of type $(2;0)$ with a singularity at the origin. This class of vector fields, endowed with the C^∞ topology, will be denoted by $\mathfrak{X}$. From now on any vector field will be a C^∞ vector field, unless we say other thing. In what follows we will state some necessary definitions.

Definition 1. *Two germs of vector fields $X, Y \in \mathfrak{X}$ are* topologically equivalent *if there are two neighborhoods U, V of the origin and a homeomorphism $h : U \to V$ which sends orbits of X to orbits of Y preserving or reversing the orientation of all orbits. The homeomorphism h is a topological equivalence between X and Y.*

Definition 2. *A germ of vector field $X \in \mathfrak{X}$ is* structural stable *if there is a neighborhood N of X such that X is topologically equivalent to every $Y \in N$. The set of the structural stable germs will be denoted by Σ_0. We will also consider the set $\mathfrak{X}_1 = \mathfrak{X} \backslash \Sigma_0$, i.e. the bifurcation set of $\mathfrak{X}$.*

Definition 3. *Let $J = [-\epsilon, \epsilon]$ be a closed interval. Denote by Θ the space of C^1 mappings $\xi : J \to \mathfrak{X}$ endowed with the C^1 topology. Its elements will be called* one-parameter families of germs of vector fields *of $\mathfrak{X}$. ξ is generic if*

1. *$\xi(-\epsilon)$, $\xi(\epsilon) \in \Sigma_0$;*
2. *there is at most one $\epsilon_0 \in J$ such that $\xi(\epsilon_0) \in \mathfrak{X}_1$ and in this case $\xi(\epsilon_0)$ is structural stable in $\mathfrak{X}_1$;*
3. *it is transversal to $\mathfrak{X}_1$.*

Definition 4. *Two one-parameter families ξ, $\eta \in \Theta$ are* topologically equivalent *if there is a reparametrization $h : J \to J$ and a family of homeomorphisms $H : J \to Hom(U, V)$, not necessarily continuous, such that for every $\lambda \in J$ we have that $H(\lambda)$ is a topological equivalence between $\xi(\lambda)$ and $\eta(h(\lambda))$.*

For more details about generic one-parameter families and bifurcation sets, see [13, 20]. Buzzi proved in [2] the following theorem about $\mathfrak{X}$.

Theorem 1. *The following statements hold.*

(a) Every structural stable germ of a vector field in $\mathfrak{X}$ is topologically equivalent to one of the following germs:
   1. *$X_1 = (x^2 - y^2, 2xy)$;*

2. $X_2 = (-x^2 - 2y^2, xy)$;
3. $X_3 = (2x^2 - y^2, xy)$;
4. $X_4 = (-x^2 - y^2, -2xy)$;
5. $X_5 = (x^2 - 2y^2, -xy)$.

(b) *For λ small enough every generic one-parameter family of germs of vector fields of $\mathfrak{X}$ is topologically equivalent to one of the following families:*

1. *Every germ given in* (a);
2. $(X_{12})_\lambda = (-\lambda x^2 - y^2 + x^4, (1-\lambda)xy)$;
3. $(X_{21})_\lambda = (\lambda x^2 - y^2 - x^4, (1+\lambda)xy)$;
4. $(X_{34})_\lambda = (\lambda x^2 + 2xy - y^2 - x^4, (\lambda-1)xy + 2y^2)$;
5. $(X_{43})_\lambda = (-\lambda x^2 + 2xy - y^2 + x^4, -(\lambda+1)xy + 2y^2)$;
6. $(X_{45})_\lambda = (\lambda x^2 - y^2 - x^4, (\lambda-1)xy)$;
7. $(X_{54})_\lambda = (-\lambda x^2 - y^2 + x^4, -(\lambda+1)xy)$;
8. $(X_{13})_\lambda = ((2+\lambda)x^2 - y^2 + x^4, -\lambda x^2 + 2xy + y^2)$;
9. $(X_{24})_\lambda = ((\lambda-1)x^2 - xy - y^2 + x^4, -\lambda x^2 - xy)$.

We note that all the germs of vector fields which appear in the statement of the previous theorem are polynomial.

Theorem 1 motivated us to classify the phase portrait of the differential vector fields which appear in its statement and thus to extend the results of [2].

Our first result provides a tool for studying periodic orbits of those vector fields.

Theorem 2. *If X is a C^1 φ-reversible vector field of type $(2;0)$ satisfying $Fix(\varphi) = \{p\}$ then there is no periodic orbit surrounding p.*

The phase portraits of the vector fields in the statement of Theorem 1 will be presented in the Poincaré disk. See subsection 2.1 for more details of the Poincaré compactification.

The next theorem summarize our results.

Theorem 3. *The following statements hold.*

(a) *The phase portraits in the Poincaré disk of the vector fields of Theorem 1 are given in Figures 1, 2, 3, 4 and 5.*
(b) *The phase portraits of X_1 and X_3 are topologically equivalent.*
(c) *The bifurcations between X_1 and X_2, X_1 and X_3, X_2 and X_4, X_3 and X_4 and between X_4 and X_5 are generic and are given, respectively, by the phase portraits of X_{12} (and X_{21}), X_{13}, X_{24}, X_{34} (and X_{43}) and X_{45} (and X_{54}) for $\lambda = 0$.*
(d) *The bifurcation between X_3 and X_5 is degenerated and is given by the phase portraits of X_{45} (for $\lambda = 1$) and X_{54} (for $\lambda = -1$).*
(e) *The path of each family through $\mathfrak{X}$ is described in Table 1.*

Remark 1. *Figures 1, 2, 3, 4 and 5 work as follow. The thicker lines represent the separatrices of the phase portrait and the thin lines represent generic orbits of the canonical regions (see subsection 2.3 for more details). The biggest dots represent isolated singularities. The dot line at X_{12} and X_{45} for $\lambda = 1$ and at X_{54} for $\lambda = -1$ represents a line of singularities.*

Remark 2. *Table 1 work as follow. The line given by X_{45} mean that X_{45} is topologically equivalent at the origin to X_1 for $\lambda > 1$; to X_4 for $\lambda \leqslant 0$; to X_5 for $0 < \lambda < 1$ and to none of the five structural stable ones for $\lambda = 1$. Although the phase portraits of X_1 and X_3 are topologically equivalent at the origin, in Table 1 we consider equivalent to X_1 the families with only two elliptical sectors at the origin. If the origin has two elliptical sectors and also some parabolic sectors then we consider it equivalent to X_3. The other lines are similar.*

Remark 3. *Although we struggled to give as many analytical proofs as possible, one shall see in Proposition 4 that dealing analytically with limit cycles is a very difficult task and therefore we point out that numerical calculations about the number of limit cycles of system X_{34} were used when the parameter $\lambda \in (1, 3)$.*

The paper is organized as follows. In section 2 we present the preliminaries. Theorem 2 is proved in section 3. In section 4 we study the phase portraits. Theorem 3 is proved in section 5.

	X_1	X_2	X_3	X_4	X_5	None
X_{12}		$0 < \lambda$	$\lambda \leqslant 0$			$\lambda = 1$
X_{21}	$0 < \lambda$	$\lambda \leqslant 0$				
X_{34}			$-1 < \lambda \leqslant 0$ $3 \leqslant \lambda$	$\lambda \leqslant -1$ $0 < \lambda < 3$		
X_{43}			$\lambda < -3$ $0 < \lambda \leqslant 1$	$-3 \leqslant \lambda \leqslant 0$ $1 < \lambda$		
X_{45}	$1 < \lambda$			$\lambda \leqslant 0$	$0 < \lambda < 1$	$\lambda = 1$
X_{54}			$\lambda < -1$	$0 < \lambda$	$-1 < \lambda \leqslant 0$	$\lambda = -1$
X_{13}		$\lambda \leqslant -1$	$-1 < \lambda$			
X_{24}		$\lambda < 0$		$0 \leqslant \lambda < 1$ $1 < \lambda$	$\lambda = 1$	

TABLE 1. Behavior of each family through $\mathfrak{X}$.

2. Preliminaries

2.1. **Poincaré Compactification.** Let X be a planar *polynomial* vector field of degree $n \in \{2, 4\}$, as our polynomial differential systems of Theorem 1. The *Poincaré compactified vector field* $p(X)$ is an analytic vector field on $\mathbb{S}^2$ constructed as follow (for more details see Chapter 5 of [6]).

First we identify $\mathbb{R}^2$ with the plane $(x_1, x_2, 1)$ in $\mathbb{R}^3$ and define the *Poincaré sphere* as $\mathbb{S}^2 = \{y = (y_1, y_2, y_3) \in \mathbb{R}^3 : y_1^2+y_2^2+y_3^2 = 1\}$. We define the *northern hemisphere*, the *southern hemisphere* and the *equator* respectively by $H_+ = \{y \in \mathbb{S}^2 : y_3 > 0\}$, $H_- = \{y \in \mathbb{S}^2 : y_3 < 0\}$ and $\mathbb{S}^1 = \{y \in \mathbb{S}^2 : y_3 = 0\}$.

Consider now the projections $f_\pm : \mathbb{R}^2 \to H_\pm$ given by $f_\pm(x_1, x_2) = \pm\Delta(x_1, x_2)(x_1, x_2, 1)$, where $\Delta(x_1, x_2) = (x_1^2 + x_2^2 + 1)^{-\frac{1}{2}}$. These two maps define two copies of X, one copy X^+ in H_+ and one copy X^- in H_-. Consider the vector field $X' = X^+ \cup X^-$ defined in $\mathbb{S}^2\backslash\mathbb{S}^1$. Note that the *infinity* of $\mathbb{R}^2$ is identified with the equator $\mathbb{S}^1$. The Poincaré compactified vector field $p(X)$ is the analytic extension of X' from $\mathbb{S}^2\backslash\mathbb{S}^1$ to $\mathbb{S}^2$ given by $y_3^{n-1}X'$. The *Poincaré disk* $\mathbb{D}$ is the projection of the closed northern hemisphere to $y_3 = 0$ under $(y_1, y_2, y_3) \mapsto (y_1, y_2)$ (the vector field given by this projection will also be denoted by $p(X)$). Note that to know the behavior $p(X)$ near $\mathbb{S}^1$ is the same than to know the behavior of X near the infinity. We define the local charts of $\mathbb{S}^2$ by $U_i = \{y \in \mathbb{S}^2 : y_i > 0\}$ and $V_i = \{y \in \mathbb{S}^2 : y_i < 0\}$ for $i \in \{1, 2, 3\}$. In these charts we define $\phi_i : U_i \to \mathbb{R}^2$ and $\psi_i : V_i \to \mathbb{R}^2$ by $\phi_i(y_1, y_2, y_3) = -\psi_i(y_1, y_2, y_3) = \left(\frac{y_m}{y_i}, \frac{y_n}{y_i}\right)$, where $m \neq i$, $n \neq i$ and $m < n$. Denoting by (u, v) the image of ϕ_i and ψ_i in every chart (therefore (u, v) will play different roles in each chart) one can see the following expressions for $p(X)$:

$$
\begin{aligned}
&v^n\, m(u,v)\left(Q\left(\frac{1}{v},\frac{u}{v}\right) - uP\left(\frac{1}{v},\frac{u}{v}\right), -vP\left(\frac{1}{v},\frac{u}{v}\right)\right) \text{ in } U_1,\\
&v^n\, m(u,v)\left(P\left(\frac{u}{v},\frac{1}{v}\right) - uQ\left(\frac{u}{v},\frac{1}{v}\right), -vQ\left(\frac{u}{v},\frac{1}{v}\right)\right) \text{ in } U_2,\\
&m(u,v)(P(u,v), Q(u,v)) \text{ in } U_3,
\end{aligned}
$$

where $m(u, v) = (u^2 + v^2 + 1)^{-\frac{1}{2}(n-1)}$. We can omit the term $m(u, v)$ by a time rescaling of $p(X)$. Therefore we obtain a polynomial expression of $p(X)$ in each U_i. The expressions of $p(X)$ in each V_i is the same as that for each U_i, except by a multiplicative factor of -1. In these coordinates for $i \in \{1, 2\}$, $v = 0$ always represents the points of $\mathbb{S}^1$ and thus the infinity of $\mathbb{R}^2$. Note that $\mathbb{S}^1$ is invariant under the flow of $p(X)$.

2.2. **Blow Up Technique.** If the origin is an isolated singularity of a *polynomial* vector field X then we can apply the change of coordinates $\phi : \mathbb{R}_+ \times \mathbb{S}^1 \to \mathbb{R}^2$ given by $\phi(\theta, r) = (r\cos\theta, r\sin\theta) = (x, y)$, where $\mathbb{R}_+ = \{r \in \mathbb{R} : r > 0\}$. Therefore we can induce a vector field X_0 in $\mathbb{R}_+ \times \mathbb{S}^1$ by pullback, i.e. $X_0 = D\phi^{-1}X$. One can see that if the k-jet of X (i.e. the Taylor expansion of order k of X, denoted by j_k) is zero at the origin then the k-jet of X_0 is also zero in every point of $\{0\} \times \mathbb{S}^1$. Thus, taking the first $k \in \mathbb{N}$ satisfying $j_k(0, 0) = 0$ and $j_{k+1}(0, 0) \neq 0$ we can define the vector field $\hat{X} = \frac{1}{r^k}X_0$. Therefore, to know the behavior of $\hat{X}$ near $\mathbb{S}^1$ is the same than to know the behavior of X near the origin. One can also see

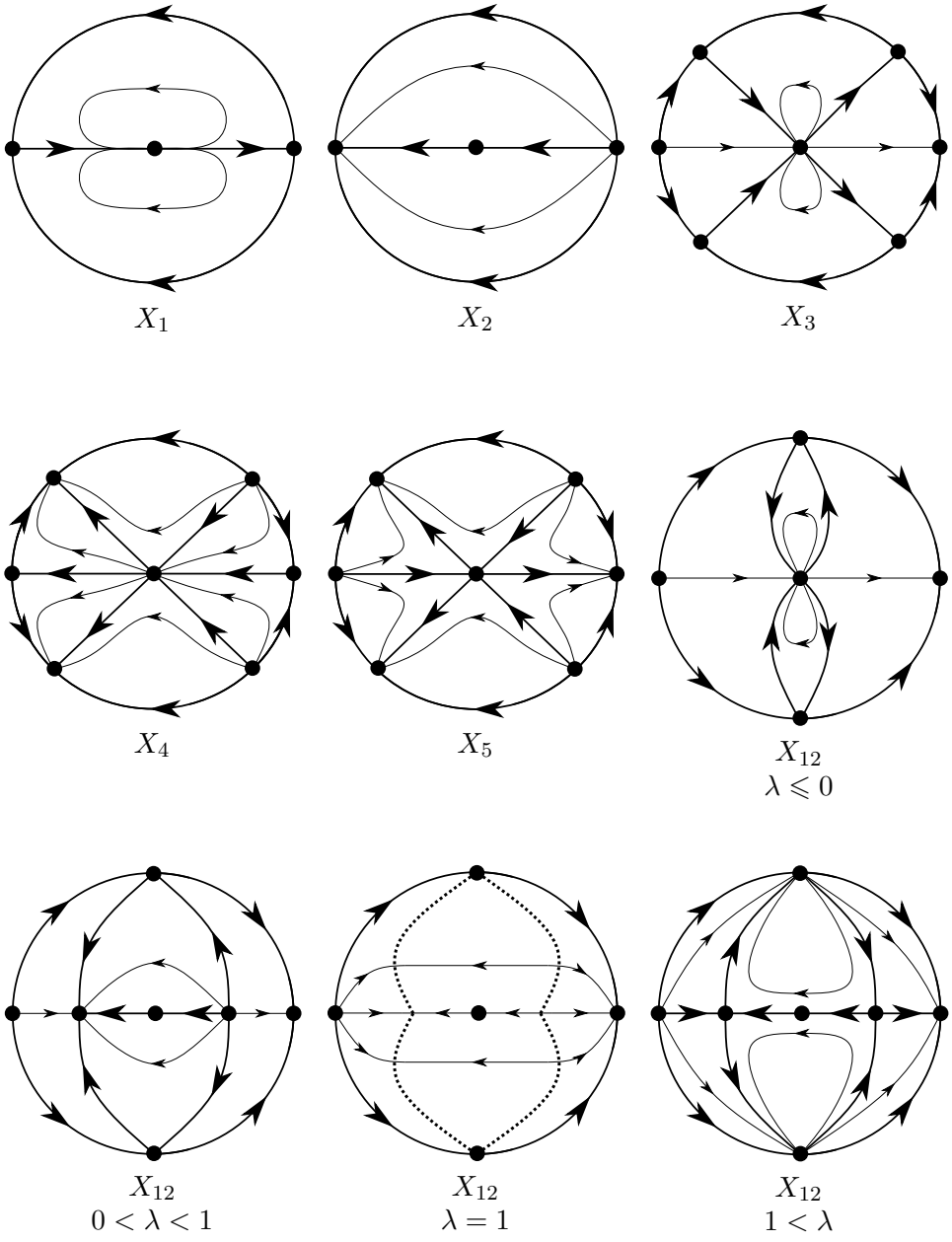

FIGURE 1. Phase portraits of X_1, X_2, X_3, X_4, X_5 and X_{12}.

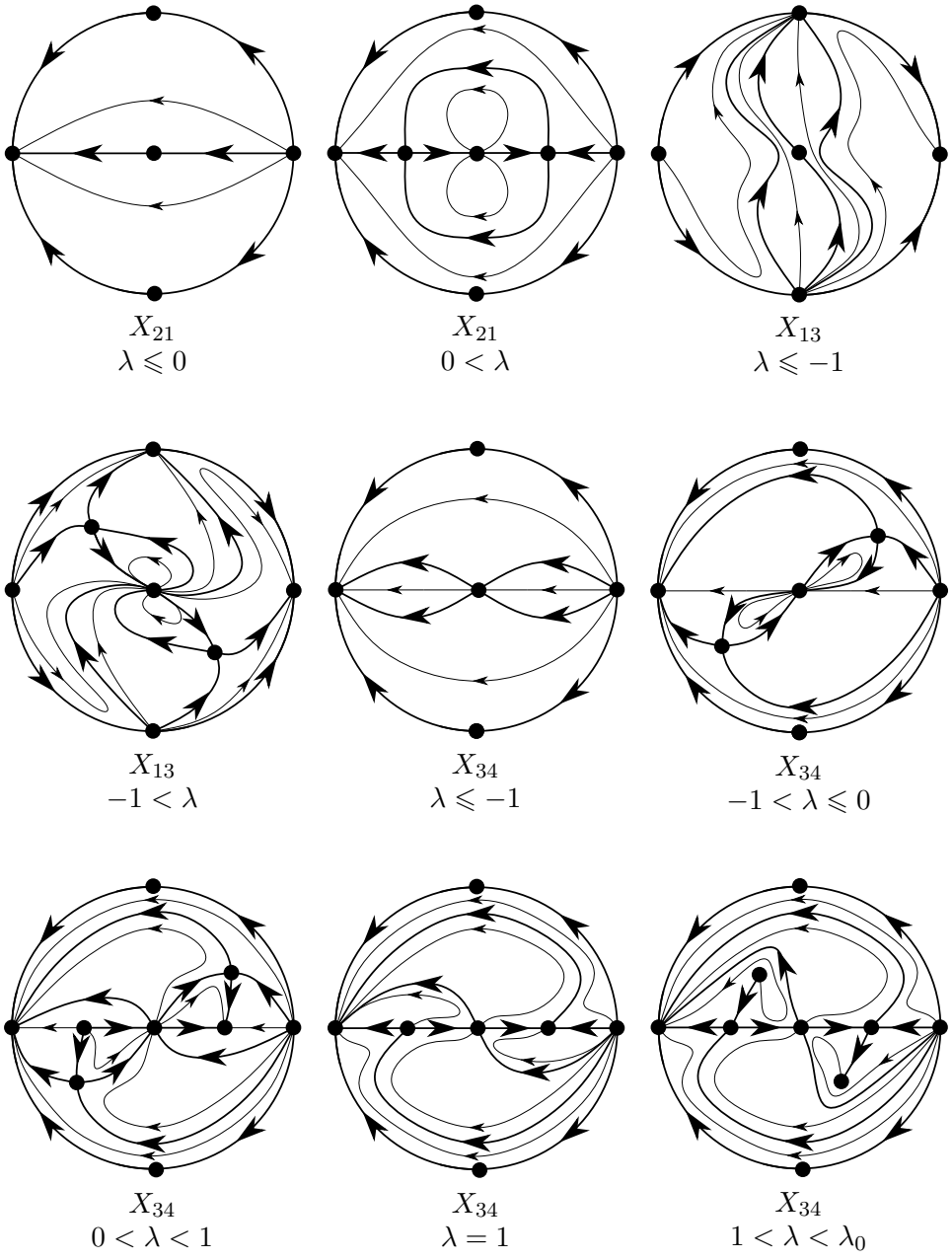

FIGURE 2. Phase portraits of X_{21}, X_{13} and X_{34}.

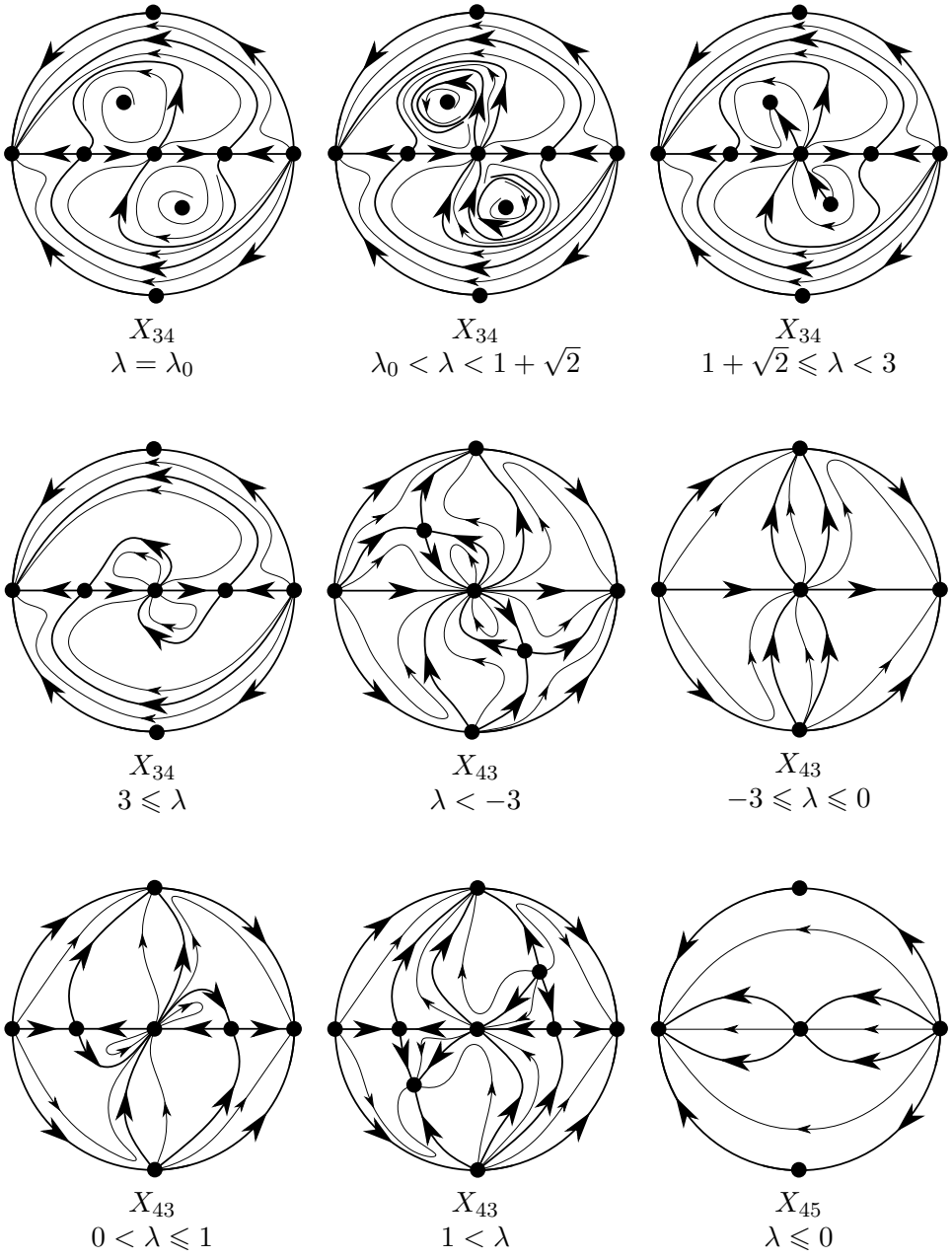

FIGURE 3. Phase portraits of X_{34}, X_{43} and X_{45}.

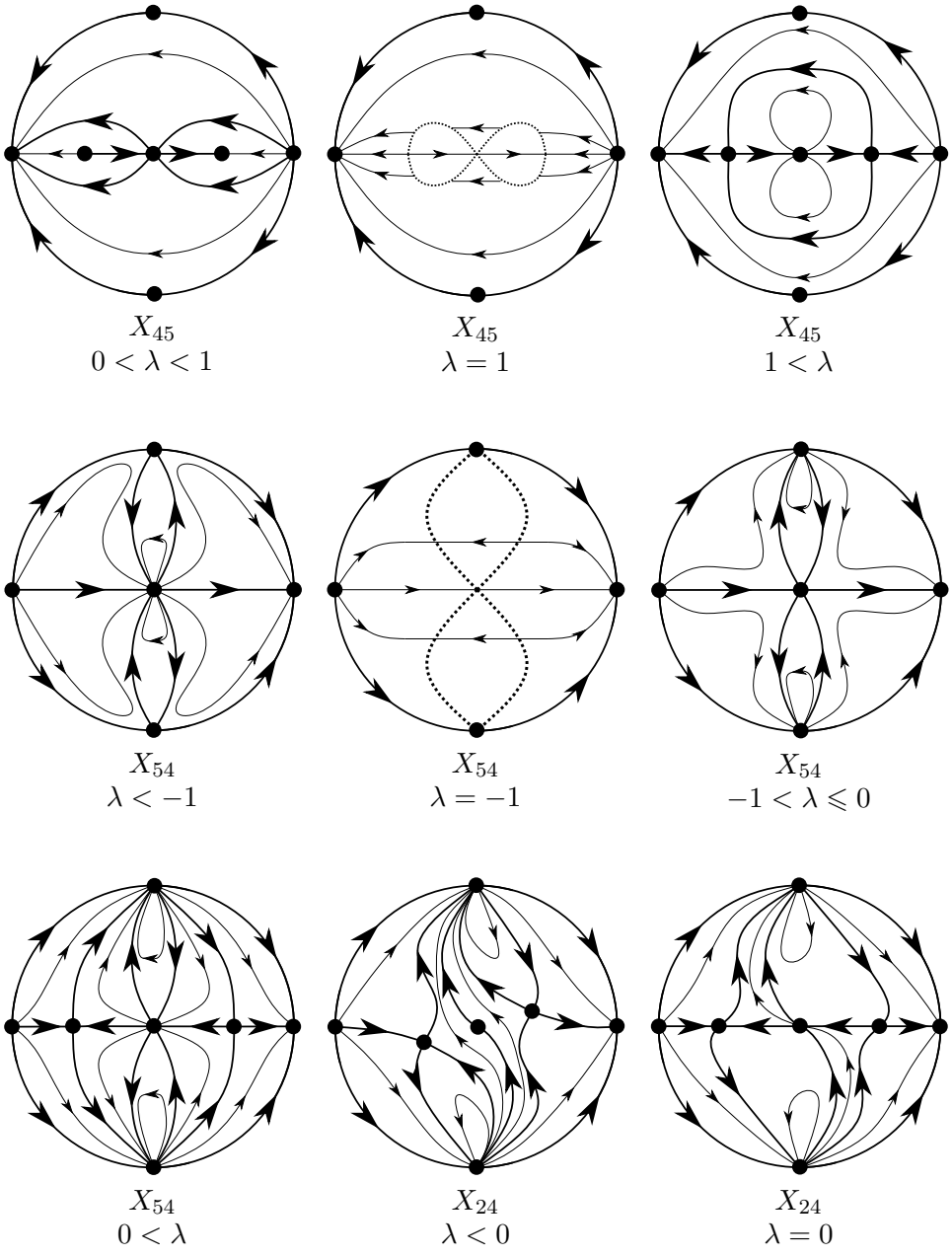

FIGURE 4. Phase portraits of X_{45}, X_{54} and X_{24}.

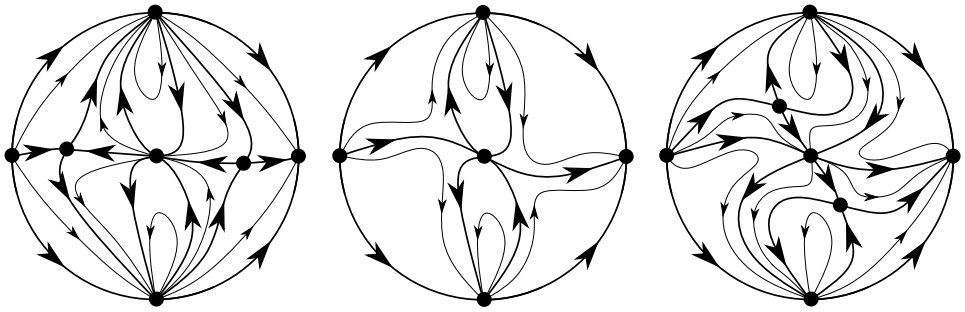

FIGURE 5. Phase portraits of X_{24}.

that $\mathbb{S}^1$ is invariant under the flow of $\hat{X}$. For a more detailed study of this technique, see Chapter 3 of [6]. One can also see that $\hat{X}$ is given by

$$\dot{r} = \frac{x\dot{x} + y\dot{y}}{r^{k+1}}, \qquad \dot{\theta} = \frac{x\dot{y} - y\dot{x}}{r^{k+2}}.$$

There is a generalization of the Blow Up Technique, known as *Quasi-homogeneous Blow Up*. This time we consider the change of coordinates $\psi(\theta, r) = (r^\alpha \cos\theta, r^\beta \sin\theta) = (x, y)$ for $(\alpha, \beta) \in \mathbb{N}^2$. Similarly to the previous technique, we can induce a vector field X_0 in $\mathbb{R}_+ \times \mathbb{S}^1$. For some $k \in \mathbb{N}$ maximal one can define $X_{\alpha,\beta} = \frac{1}{r^k} X_0$ and see that this vector field is given by

$$\dot{r} = \xi(\theta)\frac{\cos\theta\, r^\beta \dot{x} + \sin\theta\, r^\alpha \dot{y}}{r^{\alpha+\beta+k-1}}, \qquad \dot{\theta} = \xi(\theta)\frac{\alpha\cos\theta\, r^\alpha \dot{y} - \beta\sin\theta\, r^\beta \dot{x}}{r^{\alpha+\beta+k}},$$

where $\xi(\theta) = (\beta\sin^2\theta + \alpha\cos^2\theta)^{-1}$. Similarly to the previous technique, to know the behavior of $X_{\alpha,\beta}$ near $\mathbb{S}^1$ (which is invariant) is the same than to know the behavior of X near the origin. For more details see chapter 3 of [6].

2.3. **Markus-Neumann-Peixoto Theorem.** Let X be a *polynomial* vector field, $p(X)$ its compactification defined on $\mathbb{D}$ and ϕ the flow defined by $p(X)$. The separatrices of $p(X)$ are:

1. all the orbits contained in $\mathbb{S}^1$, i.e. at infinity;
2. all the singular points;
3. all the separatrices of the hyperbolic sectors of the finite and infinite singular points; and
4. all the limit cycles of X.

Denote by $\mathcal{S}$ the set of all separatrices. It is known that $\mathcal{S}$ is closed, see for instance [6]. Each connected component of $\mathbb{D}\backslash\mathcal{S}$ is called a *canonical region* of the flow $(\mathbb{D},\phi)$. The *separatrix configuration* $\mathcal{S}_c$ of a flow $(\mathbb{D},\phi)$ is the union of all the separatrices $\mathcal{S}$ of the flow together with one orbit belonging to each canonical region. The separatrix configuration $\mathcal{S}_c$ of the flow $(\mathbb{D},\phi)$ is topologically equivalent to the separatrix configuration $\mathcal{S}_c^*$ of the flow $(\mathbb{D},\phi^*)$ if there exists a homeomorphism from $\mathbb{D}$ to $\mathbb{D}$ which transforms orbits of $\mathcal{S}_c$ into orbits of $\mathcal{S}_c^*$, orbits of $\mathcal{S}$ into orbits of $\mathcal{S}^*$ and preserves or reverses the orientation of all these orbits.

Theorem 4 (Markus-Neumann-Peixoto)**.** *Let $p(X)$ and $p(Y)$ be two Poincaré compactifications in the Poincaré disk $\mathbb{D}$ of the two polynomial vector fields X and Y with finitely many singularities, respectively. Then the phase portraits of $p(X)$ and $p(Y)$ are topologically equivalent if and only if their separatrix configurations are topologically equivalent.*

For a proof of this Theorem see [7, 11, 12, 14].

In Figures 1, 2, 3, 4 and 5 we wrote the separatrix configurations of the corresponding Poincaré compactifications.

2.4. **Index of Singularities of a Vector Field.** Let p be an isolated singularity of a *polynomial* vector field X. Let e and h denote the number of elliptical and hyperbolic sectors of p, respectively. The *Poincaré index* of p is given by

$$i_p = \frac{e-h}{2} + 1.$$

It is known that $i_p \in \mathbb{Z}$. See for instance chapter 6 of [6].

Proposition 1. *Let Γ be a limit cycle of a planar polynomial vector field X. Then there is at least one singularity in the bounded region limited by it. Moreover if there is a finite number of singularities in the bounded region limited by Γ then the sum of their Poincaré index is 1.*

Theorem 5 (Poincaré-Hopf Theorem)**.** *Let X be a planar polynomial vector field and $p(X)$ its compactification defined on $\mathbb{S}^2$. If $p(X)$ has a finite number of singularities then the sum of their Poincaré index is 2.*

For a proof of Proposition 1 and Theorem 5 see chapter 6 of [6].

3. Proof of Theorem 2

Proof. The proof is by contradiction. Without loss of generality we can suppose $p = (0,0)$. Let $\gamma = \gamma(t)$ be a periodic orbit with period $T > 0$ surrounding p. There are two options: either the sets $\Gamma = \gamma([0,T])$ and $\varphi(\Gamma)$ are disjoint or not.

If Γ intersects $\varphi(\Gamma)$ then there are t_1, $t_2 \in \mathbb{R}$ satisfying $\gamma(t_1) = \varphi(\gamma(t_2))$. Define $t_3 = (t_1+t_2)/2$, $t_4 = (t_1-t_2)/2$, $\xi(t) = \gamma(t+t_3)$ and $\nu(t) = \varphi(\xi(-t))$. It is clear that ξ and ν are both solutions of X and that $\xi(t_4) = \nu(t_4)$. Therefore by the Existence and Uniqueness Theorem we have $\xi(t) = \nu(t)$ for all $t \in \mathbb{R}$. Hence $\xi(0) = \nu(0)$, i.e. $\gamma(t_3) = \varphi(\gamma(t_3))$ and therefore $\gamma(t_3) = p$, contradicting the fact that γ surrounds p.

If Γ does not intersects $\varphi(\Gamma)$ then denote by A the ring delimited by Γ and by $\varphi(\Gamma)$. Denote by U the interior of the region delimited by Γ. Once $p \in U$ it follows that $p \in \varphi(U)$. Without loss of generality we can suppose that Γ delimit the *inner boundary* of A, i.e. $\Gamma \subset \varphi(U)$. Let r be any straight line through p and $\tau : \mathbb{R} \to \mathbb{R}^2$ a parametrization of r with $\tau(0) = p$. Let $\eta_1 < 0$ be the greatest and $\eta_2 > 0$ the smallest real numbers satisfying $q_i = \tau(\eta_i) \in \Gamma$, for $i \in \{1, 2\}$. Observe that $\tau([\eta_1, \eta_2])$ does not intersects $\varphi(\Gamma)$. Define $\mu = \varphi \circ \tau$ and note that μ is continuous, $\mu(\eta_i) = \varphi(q_i)$ for $i \in \{1, 2\}$ and $\mu(0) = p$. It follows from the continuity that $\mu([\eta_1, \eta_2])$ must intersect Γ and therefore $\tau([\eta_1, \eta_2])$ must intersect $\varphi(\Gamma)$. But this contradicts the fact that $\tau([\eta_1, \eta_2])$ does not intersects $\varphi(\Gamma)$. □

4. Phase Portraits

We will show how to obtain the phase portraits of the vector field X_{34} and give a sketch of how to obtain the phase portraits of the other families. First we remember that X_{34} is given by

$$\dot{x} = \lambda x^2 + 2xy - y^2 - x^4, \qquad \dot{y} = (\lambda - 1)xy + 2y^2.$$

Note that $\{(x, y) \in \mathbb{R}^2 : \dot{y} = 0\}$ is the union of the straight lines $y = 0$ and $y = \frac{1-\lambda}{2}x$. Therefore one can see that all the possible finite singularities are given by the origin and the points

$$p^{\pm} = \pm\left(\sqrt{\lambda}, 0\right), \qquad q^{\pm} = \pm\left(\frac{1}{2}\sqrt{f(\lambda)}, \frac{1}{4}(1-\lambda)\sqrt{f(\lambda)}\right),$$

where $f(\lambda) = -(\lambda+1)(\lambda-3)$. By *possible* singularities we mean that $p^{\pm}$ are well defined only for $\lambda \geq 0$ and $q^{\pm}$ are well defined only for $-1 \leqslant \lambda \leqslant 3$. In the following three propositions we study the *local behavior* of X_{34}, i.e. we study the local phase portrait of X_{34} at each finite and infinite singularity and the existence of limit cycles for every $\lambda \in \mathbb{R}$.

Proposition 2. *For every $\lambda \in \mathbb{R}$ the following statements hold.*

- *(a) The origin is the only singularity of the chart U_1 and it is an unstable node.*
- *(b) The origin is the only singularity of the chart U_2 and its local phase portrait is given by Figure 6.*

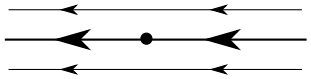

FIGURE 6. Local phase portrait at the origin of chart U_2 of $p(X_{34})$.

Proof. The first statement follows from the fact that $p(X_{34})$ is given in the chart U_1 by

$$\dot{u} = u - uv^2 + u^3v^2, \qquad \dot{v} = v - \lambda v^3 - 2uv^3 + u^2v^3.$$

To prove the second statement we will do a quasihomogeneous blow up at the origin of the chart U_2. Following the algorithm of section 3.3 of [6] we choose $(\alpha, \beta) = (1, 2)$ to apply the technique. Doing that one will obtain the vector field $X_0 = X_0(r, \theta)$ given by

$$\dot{r} = rR_1(r, \theta), \qquad \dot{\theta} = f(\theta)\sin\theta + rR_2(r, \theta),$$

where $f(\theta) \neq 0$ for all $\theta \in \mathbb{S}^1$. The linear part of X_0 at $(0, 0)$ and at $(0, \pi)$ are given by

$$DX_0(0, 0) = -DX_0(0, \pi) = \begin{pmatrix} -1 & 0 \\ 0 & 2 \end{pmatrix}.$$

Therefore all the singularities of $\mathbb{S}^1$ are hyperbolic and thus one can conclude Figure 6. □

Proposition 3. *The following statements hold.*

(a) *Singularity p^+ (resp. p^-) is a stable (resp. unstable) node for $0 < \lambda < 1$. For $1 < \lambda$ both singularities $p^\pm$ are saddles.*
(b) *Singularities $q^\pm$ are both saddles for $-1 < \lambda < 1$. For $1 < \lambda <$ 1.4314.. singularity q^+ (resp. q^-) is a stable (resp. unstable) node. For 1.4314.. $\leqslant \lambda < 1+\sqrt{2}$ singularity q^+ (resp. q^-) is a stable (resp. unstable) focus. For $1+\sqrt{2} \leqslant \lambda \leqslant$ 2.8549.. singularity q^+ (resp. q^-) is a unstable (resp. stable) focus. For 2.8549.. $< \lambda < 3$ singularity q^+ (resp. q^-) is a unstable (resp. stable) node.*
(c) *For $\lambda = 1$ we have $q^\pm = p^\pm$ and they are both saddle-nodes.*
(d) *The local phase portrait of X_{34} at the origin and its Poincaré index i are given by Figure 7.*
(e) *It occurs a Hopf bifurcation at q^+ (resp. q^-) when $\lambda = 1 + \sqrt{2}$. Moreover, there is a hyperbolic stable (resp. unstable) limit cycle surrounding q^+ (resp. q^-) for $1 + \sqrt{2} - \epsilon < \lambda < 1 + \sqrt{2}$.*

Proof. The first statement follows from

$$DX_{34}(p^+) = \begin{pmatrix} -2\lambda^{\frac{3}{2}} & 2\sqrt{\lambda} \\ 0 & (\lambda - 1)\sqrt{\lambda} \end{pmatrix}.$$

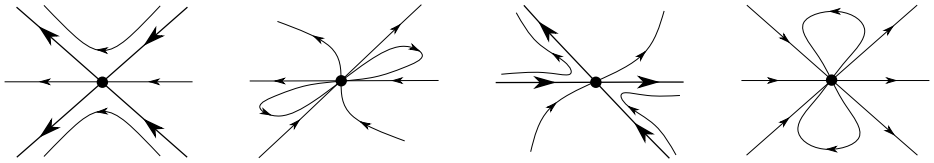

FIGURE 7. Local phase portrait of X_{34} at the origin.

Using the Theorem of Hartman-Grobman, the *Trace-Determinant Theory* (see Section 4.1 of [8]) and knowing that the determinant and the trace of $DX_{34}(q^+)$ are given, respectively, by

$$Det(\lambda) = \frac{1}{8}(\lambda+1)^2(\lambda-1)(\lambda-3)^2,$$

$$Tr(\lambda) = \frac{1}{2}\left[\lambda - \left(1-\sqrt{2}\right)\right]\left[\lambda - \left(1+\sqrt{2}\right)\right]\sqrt{f(\lambda)},$$

one can prove the second statement.

Doing the change of coordinates $(u, v) = (x-1, y)$ and then applying the blow up technique at the origin of the vector field $Y = Y(u, v)$ we obtain the vector field $Y_0 = Y_0(r, \theta)$ given by

$$\dot{r} = rR_1(r,\theta), \qquad \dot{\theta} = 2\sin\theta(\cos\theta - \sin\theta) + rR_2(r,\theta).$$

Therefore the singularities of $\mathbb{S}^1$ are given by $(r, \theta) = (0, \theta_0)$, where $\theta_0 \in \{0, \frac{\pi}{4}, \pi, \frac{5\pi}{4}\}$. Observe that

$$DY_0(0,0) = DY_0(0,\pi) = \begin{pmatrix} -2 & 0 \\ 0 & 2 \end{pmatrix},$$

$$DY_0\left(0,\frac{\pi}{4}\right) = -DY_0\left(0,\frac{5\pi}{4}\right) = \begin{pmatrix} 0 & 0 \\ * & -2 \end{pmatrix}.$$

Applying the *Center Manifold Theorem* at the non-hyperbolic points and knowing that $\dot{v} > 0$ for every point outside the u-axis we can conclude that $(0, \frac{\pi}{4})$ is a saddle and $(0, \frac{5\pi}{4})$ is a stable node for Y_0 and thus prove the third statement.

To prove the fourth statement note that the origin is a degenerated singularity, i.e. $DX_{34}(0, 0) = 0$. Doing a blow up at the origin one will obtain a vector field $X_0 = X_0(r, \theta)$ given by

$$\dot{r} = rR_1(r,\theta), \qquad \dot{\theta} = \sin\theta(\sin^2\theta - \cos^2\theta) + rR_2(r,\theta).$$

Therefore the singularities of $\mathbb{S}^1$ are given by $(r,\theta) = (0,\theta_0)$, where $\theta_0 \in \{0, \frac{\pi}{4}, \frac{3\pi}{4}, \pi, \frac{5\pi}{4}, \frac{7\pi}{4}\}$. Observe that

$$DX_0(0,0) = -DX_0(0,\pi) = \begin{pmatrix} \lambda & 0 \\ 0 & -1 \end{pmatrix},$$

$$DX_0\left(0,\frac{\pi}{4}\right) = -DX_0\left(0,\frac{5\pi}{4}\right) = \begin{pmatrix} f_1(\lambda) & 0 \\ 0 & \sqrt{2} \end{pmatrix},$$

$$DX_0\left(0,\frac{3\pi}{4}\right) = -DX_0\left(0,\frac{7\pi}{4}\right) = \begin{pmatrix} f_2(\lambda) & 0 \\ 0 & -\sqrt{2} \end{pmatrix},$$

where $f_1(\lambda) = \frac{1}{2}\sqrt{2}(\lambda+1)$ and $f_2(\lambda) = -\frac{1}{2}\sqrt{2}(\lambda-3)$. Therefore all the six singularities are hyperbolic for $\lambda \notin \{-1,0,3\}$ and thus one can conclude the local phase portrait. When $\lambda \in \{-1,0,3\}$ we have a saddle-node bifurcation at $\{(0,\frac{1}{4}\pi),(0,\frac{5}{4}\pi)\}$, $\{(0,0),(0,\pi)\}$ and $\{(0,\frac{3}{4}\pi),(0,\frac{7}{4}\pi)\}$, respectively.

The fifth statement follows from general results on the Hopf bifurcation. See for instance sections 3.4 and 3.5 of [9]. □

Proposition 4. *The vector field X_{34} may admit the existence of some limit cycle only if $\lambda \in (1,3)$. Moreover, there is a unique $\lambda_0 \in (1,3)$ in which occurs the formation of a polycicle between the origin and p^- (and p^+).*

Proof. It follows from Proposition 1 that there is at least one singularity in the interior of the bounded region limited by a limit cycle. From Theorem 2 we known that this singularity cannot be the origin. Also it cannot be singularities $p^\pm$ because the x-axis is invariant. For $-1 < \lambda < 1$ singularities $q^\pm$ are both saddles and therefore cannot have a limit cycle surrounding them because the topological index of a saddle is -1 (otherwise it must have another singularity in the bounded region limited by the limit cycle, which is impossible). Therefore if there is a limit cycle then it surrounds one (and only one) of the singularities $q^\pm$ and $1 < \lambda < 3$. From now on we will focus on the q^- singularity at the second quadrant. The dynamics at q^+ follows from the symmetry of the system.

At $\lambda = 1$ we have a saddle-node bifurcation between singularities p^- and q^-. At $\lambda = 3$ we have another saddle-node bifurcation, but now between a hyperbolic saddle at the blow up of the origin and q^-. Therefore, from the continuity of the vector field we conclude that there is a bifurcation of a heteroclinic orbit Γ_0 between the hyperbolic saddles p_0 and p^- for some value of the parameter $\lambda = \lambda_0$, see Figure 8.

Let $x_0 \in \Gamma_0$ and l_0 be a transversal section of Γ_0 passing through x_0. Following [19] we define n to be the coordinate along the normal line l_0 such that $n > 0$ outside the polycycle and $n < 0$ inside the polycycle. We also denote by Γ^s_λ and Γ^u_λ the perturbations of Γ_0, for $|\lambda - \lambda_0|$ small enough, such that $\omega(\Gamma^s_\lambda) = p^-$ and $\alpha(\Gamma^u_\lambda) = (0,0)$. Let x^s_λ and x^u_λ be the intersection of Γ^s_λ and Γ^u_λ with l_0 and $n^s(\lambda)$, $n^u(\lambda)$ its coordinates along l_0, respectively. We

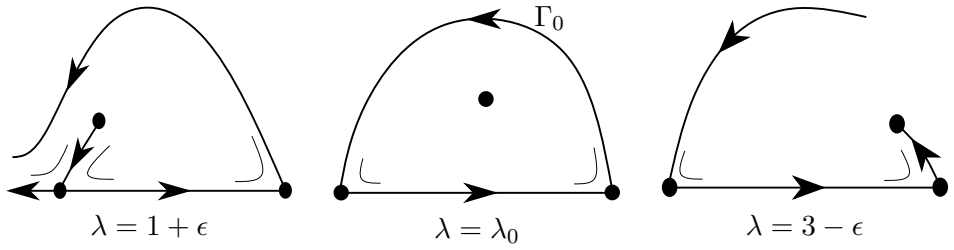

FIGURE 8. Heteroclinic orbit between the origin and p^-.

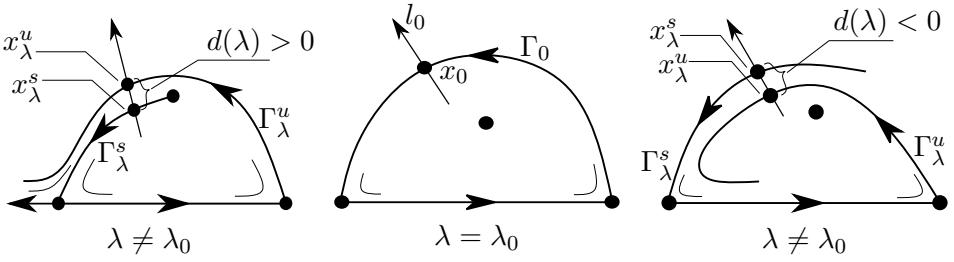

FIGURE 9. The displacement function $d(\lambda)$ defined for λ near λ_0.

define the displacement function $d(\lambda) = n^u(\lambda) - n^s(\lambda)$. See Figure 9. Let $\gamma(t)$ be a parametrization of Γ_0, with $\gamma(0) = x_0$, and $f(t;\lambda) = X_{34}(\gamma(t);\lambda)$. It follows from [19] that

$$d'(\lambda_0) = -\frac{1}{|f(0;\lambda_0)|}\int_{-\infty}^{+\infty}\left(e^{-\int_0^t Div(f(s;\lambda_0))\,ds}\right) f(t;\lambda_0) \wedge \frac{\partial f}{\partial \lambda}(t;\lambda_0)\,dt,$$

where $(x_1,x_2)\wedge(y_1,y_2) = x_1y_2 - x_2y_1$. One can see that

$$X_{34}(x,y;\lambda) \wedge \frac{\partial X_{34}}{\partial \lambda}(x,y;\lambda) = x^3y - xy^3 - x^5y = H(x,y).$$

Therefore the set $\{(x,y) \in \mathbb{R}^2 : H(x,y) = 0\}$ is given by the union of the graphs of $y = 0$ and $y = \pm\sqrt{x^2 - x^4}$. We denote $y_1(x) = \sqrt{x^2 - x^4}$ when $-1 \leqslant x \leqslant 0$. The graph of y_1 is given by the solid line of Figure 10. The dashed line denotes the points which satisfy $\dot{x} = 0$, given explicitly by $y = x\left(1 - \sqrt{\lambda + 1 - x^2}\right)$ when $-\sqrt{\lambda} \leqslant x \leqslant 0$. One can see that the flow of X_{34} is transversal to the graph of y_1, except at $q^- = (q_1, q_2)$, for every $1 < \lambda < 3$. Moreover it points outwards for $x > q_1$ and inwards for $x < q_1$. One can also see that H, inside the second quadrant, is positive at the unbounded region delimited by the graph of y_1 and negative at the bounded region. The Taylor series of y_1 at $x = 0$ is given by

$$y_1(x) = -x + 3x^3 + O(x^5).$$

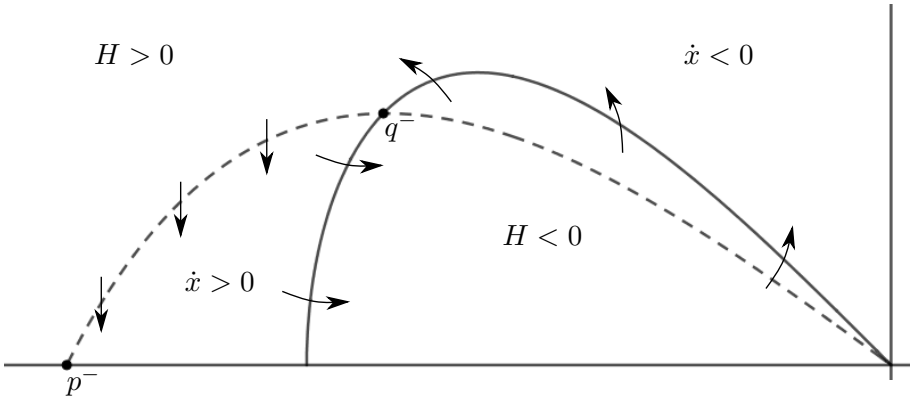

FIGURE 10. Plot of $H(x, y) = 0$ and $\dot{x} = 0$ at the second quadrant.

On the other hand the separatrix Γ_0 is given, for $|x|$ small, by

$$y_2(x) = -x + \frac{1}{8 - 2\lambda}x^3 + O(x^5).$$

Therefore for $x < 0$ small enough we have

$$y_2(x) - y_1(x) = \left(\frac{1}{8 - 2\lambda} - 3\right) x^3 + O(x^5).$$

Hence the heteroclinic orbit Γ_0 is above the graph of y_1 and therefore we conclude that

$$f(t; \lambda_0) \wedge \frac{\partial f}{\partial \lambda}(t; \lambda_0) > 0$$

for every $t \in \mathbb{R}$, independently of the exactly value of λ_0. Hence $d'(\lambda_0) < 0$. Thus we conclude that if a heteroclinic orbit Γ_0 exists at $\lambda = \lambda_0$ then for $|\lambda - \lambda_0|$ small enough the displacement function is well defined and is given by

$$d(\lambda) = a_1(\lambda - \lambda_0) + O((\lambda - \lambda_0)^2),$$

with $a_1 < 0$. Therefore we have $d(\lambda) > 0$ if $\lambda < \lambda_0$ and $d(\lambda) < 0$ if $\lambda > 0$. See Figure 9. And this happens independently of the value of λ_0. Hence there is a unique $\lambda_0 \in (1, 3)$ for which Γ_0 exists. □

If Γ_n is a polycycle with n hyperbolic saddles such that $\mu_i < 0 < \nu_i$ are its eigenvalues, then we say that Γ_n is simple if

$$H(\Gamma_n) = \prod_{i=1}^{n} \frac{|\mu_i|}{\nu_i} \neq 1.$$

Moreover Γ_n is stable if $H(\Gamma_n) > 1$ and unstable if $H(\Gamma_n) < 1$. See for instance [3, 5, 21]. The polycycle Γ that bifurcate at $\lambda = \lambda_0$ is formed by p^-

and from two hyperbolic saddles from the blow up of the origin. Hence one can calculate that

$$H(\Gamma_0) = \frac{\lambda - 1}{3 - \lambda}.$$

To precise in an analytical way how many limit cycles exists in a given interval in general is a very difficult task. But numerical computations (see chapters 9 and 10 of [6]) points that $\lambda_0 = 2.3761..$ and thus Γ is stable. Moreover the numerical computations also indicates that there is no limit cycles for $\lambda \in (1, \lambda_0) \cup (1 + \sqrt{2}, 3)$ and that there is a unique limit cycle for $\lambda \in (\lambda_0, 1 + \sqrt{2})$. So to provide an analytic proof of these two facts is an open problem. Knowing this, it follows from [18] that the limit cycle which ends at the Hopf bifurcation belongs to an open maximal family of limit cycles which born at the polycicle for $\lambda = \lambda_0$.

In what follows we will study some cases of X_{34}. The other cases can be obtained similarly.

Proposition 5. *The phase portrait of X_{34} for $1 + \sqrt{2} \leqslant \lambda < 3$ is the one in Figure 3.*

Proof. From Propositions 2, 3, 4 and from the invariance of the x-axis we can conclude Figure 11. To simplify the writing we will name the infinite

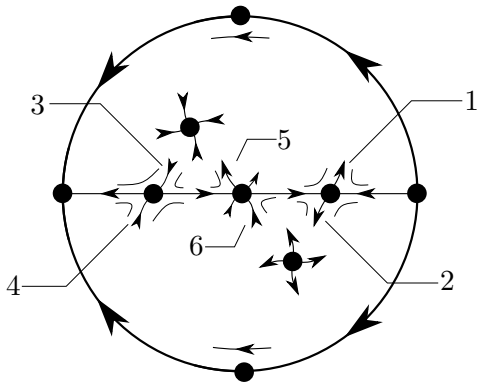

FIGURE 11. Unfinished phase portrait of X_{34} for $1 + \sqrt{2} \leqslant \lambda < 3$.

singularities by *north pole*, *south pole*, *east pole* (right) and *west pole* (left). We claim that separatrix 1 must have the west pole as its ω-limit. To prove this consider Figure 12. Denote $S = \{(x, y) \in \mathbb{R}^2 : \dot{x} = 0\}$ and observe that it is given explicitly by

$$y = x \pm \sqrt{x^2(\lambda + 1) - x^4}.$$

Observe that separatrix 1 must cross the y-axis because all its options for ω-limit are at the second quadrant. At the bounded region limited by S we

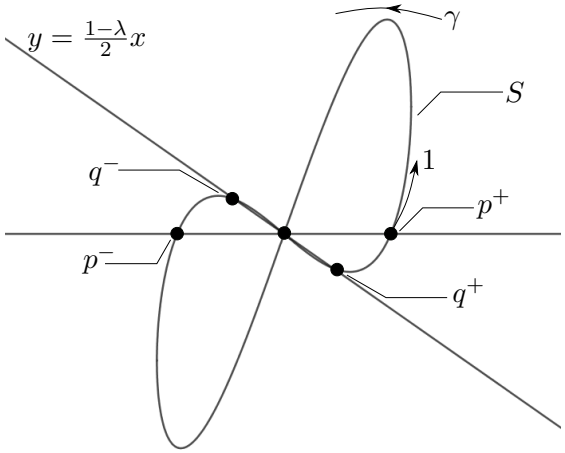

FIGURE 12. Illustration of the zeros of $\dot{x} = 0$ and $\dot{y} = 0$.

have $\dot{x} > 0$, therefore separatrix 1 must pass above S, at least somewhere near γ. Observe that this does not depend if separatrix 1 is tangential or not with S. One can prove using the *Lagrange Multipliers* that the maximum value of y at S is given by

$$y_0 = \frac{\sqrt{2}}{8}\left(2\sqrt{3+4\lambda+\sqrt{9+8\lambda}} + \sqrt{3+12\lambda+8\lambda^2+\sqrt{9+8\lambda}}\right).$$

At the region limited by $y > 0$ and $y > \frac{1-\lambda}{2}x$ we have $\dot{y} > 0$ and therefore separatrix 1 will cross the straight line given by $y = \frac{1-\lambda}{2}x$ at a point (x_1, y_1) such that $y_1 > y_0$. This is enough to ensure that separatrix 1 cannot end at separatrix 3 nor at the stable node because $\dot{x} < 0$ at the unbounded region delimited by S. Therefore separatrix 1 ends at the west pole and q^- is in the bounded region limited by it. Separatrix 3 has no other option than born at the origin. Once the stable node (i.e. the singularity q^-) came from a saddle-node bifurcation at the origin at $\lambda = 3$ we conclude that separatrix 5 end at this node. The symmetry of the system is now enough to finish the phase portrait. □

Proposition 6. *The phase portrait of X_{34} for $\lambda_0 < \lambda < 1 + \sqrt{2}$ is the one given by Figure 3.*

Proof. Similarly to Proposition 5, here we conclude Figure 13 and the fact that separatrix 1 also end at the west pole with the limit cycle in the bounded region delimited by it. Follows from Proposition 5 and the continuity of X_{34} with respect to λ that separatrix 3 must end at the limit cycle. Separatrix 5 has no other option than born at the origin. Symmetry is now enough to finish the phase portrait. □

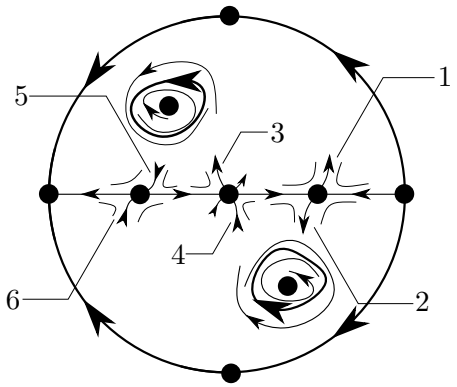

FIGURE 13. Unfinished phase portrait of X_{34} for $\lambda_0 < \lambda < 1+\sqrt{2}$.

Proposition 7. *The phase portrait of X_{34} for $1 < \lambda < \lambda_0$ is the one given by Figure 2.*

Proof. Similarly to Propositions 5 and 6, here we conclude Figure 14 and the fact that separatrix 1 also end at the west pole with the unstable node (i.e. the singularity q^-) in the bounded region delimited by it. Once we

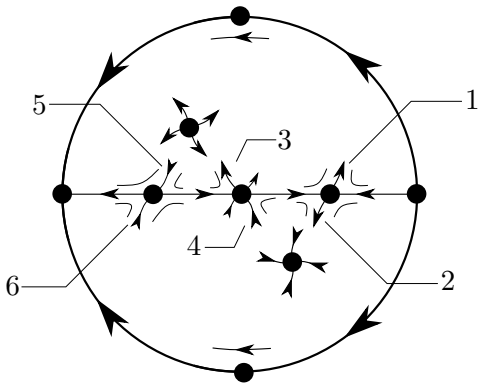

FIGURE 14. Unfinished phase portrait of X_{34} for $1 < \lambda < \lambda_0$.

have a generic saddle-node bifurcation at $\lambda = 1$ we conclude that separatrix 5 born at the unstable node. Separatrix 3 has no other option than end at the west pole. Symmetry is now enough to finish the phase portrait. □

Proposition 8. *The phase portrait of X_{34} for $0 < \lambda < 1$ is the one given by Figure 2.*

Proof. Similarly to Proposition 5, 6 and 7 in this case we have Figure 15. Observe that $\dot{x} = -y^2$ if $x = 0$, therefore no orbit can cross the y-axis from

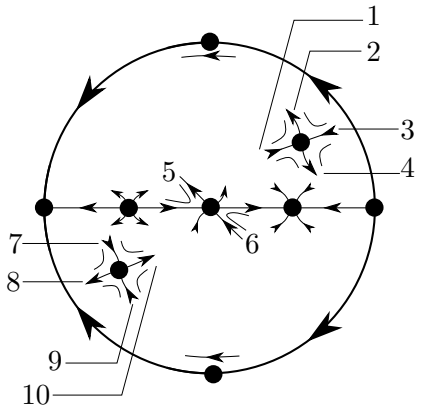

FIGURE 15. Unfinished phase portrait of X_{34} for $0 < \lambda < 1$.

left to right. Remember that $y = \frac{1-\lambda}{2}x$ imply $\dot{y} = 0$ and thus we conclude Figure 16. Observe that separatrix 2 cannot end at separatrix 1 nor at

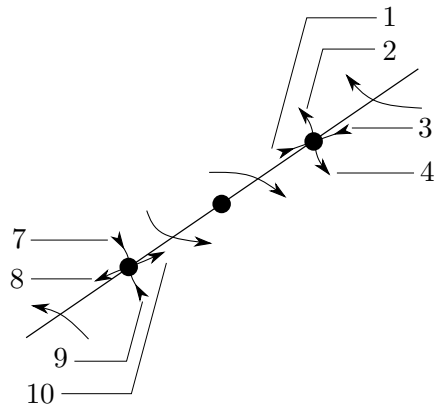

FIGURE 16. Local phase portrait of X_{34} at $y = \frac{1-\lambda}{2}x$ for $0 < \lambda < 1$.

separatrix 3, otherwise it would have a singularity in the bounded region limited by it. If separatrix 2 ends at stable node then by Figure 16 separatrix 1 could not born anywhere. Therefore the only option to separatrix 2 is to end at the west pole. Separatrix 4 must end at the stable node because we have a generic saddle-node bifurcation. There is no other option for separatrix 3 other than born at the east pole. The fact that no orbit can cross the y-axis from left to right give to separatrix 1 no other option than born at the origin (not at separatrix 5). Separatrix 5 cannot cross the y-axis, therefore it must end at the west pole. Symmetry is now enough to finish the phase portrait. □

Remark 4. *The proofs for $\lambda \leqslant 0$ and $3 \leqslant \lambda$ are similarly as Propositions 5, 6, 7 and 8.*

Remark 5. *Theorem 2 together with observations as the invariance of the x-axis, the fact that the index of a saddle is -1 and the Bendixson criterion proves the nonexistence of any limit cycles at the others families of vector fields.*

Proposition 9. *The phase portrait of X_{12} for $\lambda \in \mathbb{R}$ are those given by Figure 1.*

Proof. Once $\dot{y} = 0$ if, and only if $x = 0$ or $y = 0$ or $\lambda = 1$ one can see that the only possible finite singularities are the origin and the points $p^{\pm} = \pm(\sqrt{\lambda}, 0)$ if $\lambda \neq 1$, and the algebraic curve $-x^2 - y^2 + x^4 = 0$ if $\lambda = 1$. Doing a blow up at the origin and knowing that

$$DX_{12}(p^+) = \begin{pmatrix} 2\lambda^{\frac{3}{2}} & 0 \\ 0 & (1-\lambda)\sqrt{\lambda} \end{pmatrix},$$

one can understand the *local behavior* of X_{12}, similarly as we did with X_{34}. At the infinite one will see that the only singularities are the origins of each chart. The origin of the chart U_1 (the east pole) is a stable node for every $\lambda \in \mathbb{R}$. The origin of the chart U_2 requires a blow up. First note that the field $p(X_{12})$ at this chart is given by

$$\dot{u} = -v^2 + u^4 - u^2v^2, \qquad \dot{v} = (\lambda - 1)uv^3.$$

Assume $\lambda \neq 1$. Doing a quasihomogeneous blow up with $(\alpha, \beta) = (1, 2)$ one will see that the only singularities of our interest (i.e. those with $r = 0$) are given by the zeros of

$$\sin\theta(\cos^4\theta - \sin^2\theta) = 0,$$

for $0 \leqslant \theta < 2\pi$. There are six singularities, given by $\theta = 0$, $\theta = \pi$ and $\theta = \theta_i$, $i \in \{1, 2, 3, 4\}$, where θ_i is the solution of $\cos^4\theta = \sin^2\theta$ at the i-th quadrant of $\mathbb{S}^1$. The linear part of the vector field $X_0 = X_0(r, \theta)$ in each of these singularities are given by

$$DX_0(0,0) = \begin{pmatrix} 1 & 0 \\ 0 & -2 \end{pmatrix}, \; DX_0(0,\theta_1) = \begin{pmatrix} 0 & 0 \\ 0 & \eta \end{pmatrix},$$

$$DX_0(0,\theta_2) = \begin{pmatrix} 0 & 0 \\ 0 & -\eta \end{pmatrix}, \; DX_0(0,\pi) = \begin{pmatrix} -1 & 0 \\ 0 & 2 \end{pmatrix},$$

$$DX_0(0,\theta_3) = \begin{pmatrix} 0 & 0 \\ 0 & -\eta \end{pmatrix}, \; DX_0(0,\theta_4) = \begin{pmatrix} 0 & 0 \\ 0 & \eta \end{pmatrix},$$

where $\eta = 4\sqrt{\sqrt{5} - 2}$. Using the *Hartman-Grobman Theorem* at $(0, 0)$ and $(0, \pi)$ and the *Center Manifold Theorem* at $(0, \theta_i)$, for $i \in \{1, 2, 3, 4\}$ one can obtain Figure 17(a). Remember that $\dot{v} = (\lambda - 1)uv^3$ and therefore

$$sign(\dot{v}) = sign(\lambda - 1)sign(u)sign(v),$$

where $sign(x)$ denotes the *signal* of x, i.e. $sign(x) = -1$ if $x < 0$, $sign(x) = 0$ if $x = 0$ and $sign(x) = 1$ if $x > 0$. Therefore we can complete Figure 17(a),

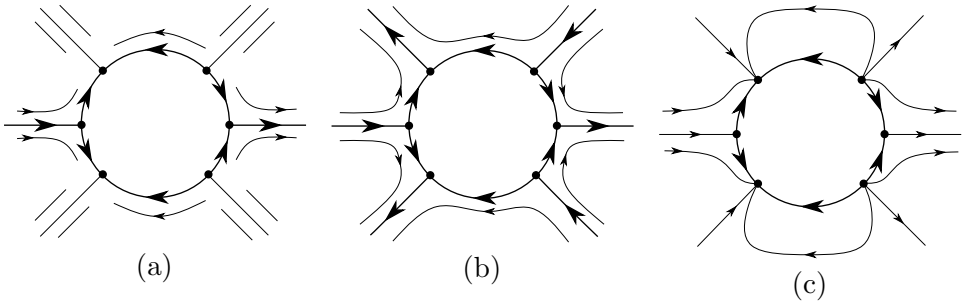

FIGURE 17. Local phase portrait of the blow up of the origin of chart U_2.

obtaining Figure 17(b) for $\lambda < 1$ and Figure 17(c) for $\lambda > 1$. Observe that $\dot{x} \leqslant 0$ if $y = 0$. The invariance of the x-axis does not permit any limit cycle here. With this informations one can obtain the phase portrait of X_{12} similarly as we did with X_{34}. When $\lambda = 1$ the equation of the vector field X_{12} becomes

$$\dot{x} = -x^2 - y^2 + x^4, \qquad \dot{y} = 0.$$

So all the straight lines $y = constant$ are invariant and the algebraic curve $-x^2 - y^2 + x^4 = 0$ is filled up with singularities. □

Proposition 10. *The phase portrait of X_{21} for $\lambda \in \mathbb{R}$ are those given by Figure 2.*

Proof. First assume $\lambda \neq -1$. Observe that the only possible singularities are the origin and the points $p^{\pm} = \pm(\sqrt{\lambda}, 0)$. With a blow up at the origin and an analysis of $DX_{21}(p^{\pm})$ one can conclude the *local behavior* of X_{21}. At the infinity only the origins of the charts are singularities. The origin of U_1 is an unstable node and a quasihomogeneous blow up with $(\alpha, \beta) = (1, 2)$ at the origin of U_2 is necessary. But in this case the analysis of this blow up is much more simple than the last one. Finally, observe that X_{21} is also reversible with $\varphi(x, y) = (-x, y)$, i.e. it is reversible in respect to the y-axis and that no limit cycle can exist due to the invariance of the x-axis. Also observe that $\dot{x} < 0$ if $x = 0$. When $\lambda = -1$ the equation of the vector field X_{21} becomes

$$\dot{x} = -x^2 - y^2 - x^4, \qquad \dot{y} = 0,$$

so all the straight lines $y = constant$ are invariant. Note that the only finite singularity is the origin because the algebraic curve $-x^2 - y^2 - x^4 = 0$ is degenerated. □

Proposition 11. *The phase portrait of X_{43} for $\lambda \in \mathbb{R}$ are those given by Figure 3.*

Proof. Note that the zeros of $\dot{y} = 0$ are given by $y = 0$ and $y = \frac{1+\lambda}{2}x$. The finite singularities are the origin and the points

$$p^{\pm} = \left(\pm\sqrt{\lambda}, 0\right), \qquad q^{\pm} = \pm\left(\frac{1}{2}\sqrt{f(\lambda)}, \frac{1}{4}(1+\lambda)\sqrt{f(\lambda)}\right),$$

where $f(\lambda) = (\lambda+3)(\lambda-1)$. An analysis of DX_{43} at $p^{\pm}$ and $q^{\pm}$ and a blow up at the origin is enough to obtain the *local behavior* of X_{43}. The origin of the chart U_1 is a stable node and the origin of U_2 requires an analysis similar to the vector field X_{12}. The nonexistence of limit cycles can be proved similarly as we did in Proposition 4. Finally, note that $\dot{x} < 0$ if $x = 0$ and an analysis (as we did in Proposition 8) of the flow on the straight line $y = \frac{1+\lambda}{2}x$ is necessary to complete the phase portrait. □

Proposition 12. *The phase portrait of X_{45} for $\lambda \in \mathbb{R}$ are those given by Figure 3 and 4.*

Proof. The only finite singularities are the origin and the points $p^{\pm} = \pm(\sqrt{\lambda}, 0)$. A blow up at the origin and an analysis of $DX_{45}(p^{\pm})$ is enough to know the *local behavior* of X_{45}. The origin of the chart U_1 is a unstable node for every $\lambda \in \mathbb{R}$ and the origin of the chart U_2 requires a quasihomogeneous blow up with $(\alpha, \beta) = (1, 2)$. The analysis of this blow up is simple and there is no other infinite singularity for this vector field. The invariance of the x-axis does not permit any limit cycle here. Finally, note that X_{45} is also invariant with $\phi(x, y) = (-x, y)$ and that $\dot{x} < 0$ if $x = 0$. □

Proposition 13. *The phase portrait of X_{54} for $\lambda \in \mathbb{R}$ are those given by Figure 4.*

Proof. The only finite singularities are the origin and the points $p^{\pm} = \pm(\sqrt{\lambda}, 0)$. As before, a blow up at the origin and an analysis of DX_{54} is enough to describe the *local behavior* of X_{54}. The origins of the charts are only infinite singularities. The origin of U_1 is a stable node and the origin of U_2 requires a quasihomogeneous blow up, with $(\alpha, \beta) = (1, 2)$, and an analysis similarly as we did with X_{12}. The invariance of the x-axis does not let any limit cycle to exist. Finally, observe that $\dot{x} < 0$ if $x = 0$ and that X_{54} is invariant with $\varphi(x, y) = (-x, y)$. □

Proposition 14. *The phase portrait of X_{13} for $\lambda \in \mathbb{R}$ are those given by Figure 2.*

Proof. First observe that

$$\dot{y} = \left[y + \left(1 + \sqrt{\lambda+1}\right)x\right]\left[y + \left(1 - \sqrt{\lambda+1}\right)x\right].$$

Knowing this one can see that the only finite singularities are the origin and the points

$$p^{\pm} = \pm\left(\sqrt{2}\sqrt[4]{\lambda+1}, -\left(1+\sqrt{\lambda+1}\right)\sqrt{2}\sqrt[4]{\lambda+1}\right).$$

An analysis of the determinant of $DX_{13}(p^{\pm})$ is enough to describe the local phase portrait of X_{13} at these singularities. A blow up at the origin is necessary. At this case the singularities of the blow up are given by the zeros of

$$-\lambda\cos^3\theta - \lambda\cos^2\theta\sin\theta + \cos\theta\sin^2\theta + \sin^3\theta = 0,$$

which are given by

$$\frac{3\pi}{4},\ \frac{7\pi}{4},\ \pm\arctan\sqrt{\lambda}\ \text{ and } \pi \pm \arctan\sqrt{\lambda}.$$

Therefore a non usual number of bifurcations will occur at the origin. But they are all very simple and almost never changes the phase portrait. The infinite singularities are given by the origins of the charts. The origin of U_1 is a stable node. As we did in X_{12}, a quasihomogeneous blow up with $(\alpha,\beta) = (1,2)$ is required for the origin of U_2. The nonexistence of limit cycles can be prove similarly as we did in Proposition 4. Observe that $\dot{x} < 0$ if $x = 0$. Finally, an analysis of the flow on the straight line $y = -(1+\sqrt{\lambda+1})x$ is necessary to complete the phase portraits. □

Proposition 15. *The phase portrait of X_{24} for $\lambda \in \mathbb{R}$ are those given by Figure 4 and 5.*

Proof. First note that the zeros of $\dot{y} = 0$ are the union of the straight lines $x = 0$ and $y = -\lambda x$. Therefore the only finite singularities are the origin and the points

$$p^{\pm} = \pm(\lambda - 1, -\lambda(\lambda - 1)).$$

An analysis of the determinant of $DX_{24}(p^{\pm})$ is enough to describe the local behavior of the singularities $p^{\pm}$. A blow up at the origin is necessary. Similarly to X_{13} the singularities are given by

$$\frac{3\pi}{4},\ \frac{7\pi}{4},\ \pm\arctan\sqrt{\lambda}\ \text{ and } \pi \pm \arctan\sqrt{\lambda}.$$

Once more the infinite singularities are the origins of the charts. The origin of U_1 is a stable node. A quasihomogeneous blow up, with $(\alpha,\beta) = (1,2)$, is necessary at the origin of U_2 and the analysis is similarly to X_{12}. An analysis of the straight line $y = -\lambda x$, as we did at Proposition 8, is necessary at every case. Finally, follows from the blow up at the origin that for $0 < \lambda < 1$ and for $1 < \lambda$ that the separatrix at the fourth quadrant of the hyperbolic sector of the origin is always tangent to the line $y = -x$, which is, respectively, *bellow* and *above* the straight line given by $y = -\sqrt{\lambda}x$, for $x > 0$. Therefore the flow at this last straight line must be analyzed to complete the phase portrait. □

Proposition 16. *The phase portrait of X_1, X_2, X_3, X_4 and X_5 are those given by Figure 1.*

Proof. No bifurcations occurs at any of this five vector fields. The origin is always the unique finite singularity. A blow up is enough to describe their local phase portrait at the origin. The nonexistence of limit cycles follows from Theorem 2. Every infinite singularity is hyperbolic. Finally, note that the straight lines $y = \pm x$ are invariant by X_3, X_4 and X_5. □

5. Proof of Theorem 3

Proof. The first statement follows from Section 4.

The second statement follows from the phase portrait of X_{13}. Although it bifurcates from X_1 to X_3 at $\lambda = 0$ its phase portrait does not change topologically for $\lambda > -1$.

To prove the third statement observe that Theorem 1, statement *(b)*, says that any bifurcation of X_{ij} for $\lambda = 0$ is generic. Therefore it is only necessary to know which bifurcations occurs from each X_{ij} at $\lambda = 0$ (the families were named after this).

The fourth statement follows from the phase portrait of X_{45} and X_{54}.

Once we know the phase portrait of every family described in Theorem 1 one can prove the fifth statement with an analysis of each family. □

6. Conclusion

To prove in a analytical way every bifurcation that can happen at a given vector field X sometimes is a very difficult task, see for instance the hundreds of papers about the bifucations of limit cycles and heteroclinic or homoclinic connections between saddles. Therefore although we struggle to give as many analytical proofs as possible, to deal in an analytical way with the number of limit cycles is a very difficult task and thus the appeal for some numerical computations was inevitable in the system here studied. Furthermore we point out that the technique of choosing convenient curves and observing how the flow crosses them has been a good tool for the analytical proofs of this paper.

Acknowledgments

We thank to the reviewers their comments and suggestions which help us to improve the presentation of this paper.

The first author is partially supported by São Paulo Research Foundation (FAPESP) grant 2019/10269-3, CAPES grant 88881.068462/2014-01 and

CNPq grant 304798/2019-3. The second author is partially supported by the Ministerio de Economía, Industria y Competitividad, Agencia Estatal de Investigación grant MTM2016-77278-P (FEDER) and PID2019-104658GB-I00 (FEDER), the Agència de Gestió d'Ajuts Universitaris i de Recerca grant 2017SGR1617, and the H2020 European Research Council grant MSCA-RISE-2017-777911. The third author is supported by São Paulo Research Foundation (FAPESP), grants 2018/23194-9 and 2019/21446-3.

References

[1] J. C. Artés and J. Llibre, *Quadratic Hamiltonian vector fields*, J. Differential Equations, 107 (1994), pp. 80-95.

[2] C. A. Buzzi, *Generic one-parameter families of reversible vector fields*, in Real and complex singularities (São Carlos, 1998), vol. 412 Chapman & Hall/CRC Res. Notes Math, Chapman & Hall/CRC, Boca Raton, FL 2000, pp. 202-214.

[3] L. A. Cherkas, *The stability of singular cycles*, Differentsial'nye Uravneniya, 4 (1968), pp. 1012-1017.

[4] J. A. C. da Rocha Medrado and M. A. Teixeira, *Symmetric singularities of reversible vector fields in dimension three*, vol. 112, 1998, pp. 122-131. Time-reversal symmetry in dynamical systems (Coventry, 1996).

[5] H. Dulac, *Sur les cycles limites*, Bull. Soc. Math. France, 51 (1923), pp. 45-188.

[6] F. Dumortier, J. Llibre and J. C. Artés, *Qualitative theory of planar differential systems*, Universitext, Springer-Verlag, Berlim, 2006.

[7] J. G. Espín Buendía and V. Jiménez López, *On the Markus-Neumann theorem*, J. Differential Equations, 265 (2018), pp. 6036-6047.

[8] M. W. Hirsch, S. Smale and R. L. Devaney, *Differential equations, dynamical systems, and an introduction to chaos*, vol. 60 of Pure and Applied Mathematics (Amsterdam), Elsevier/Academic Press, Amsterdam, second ed, 2004.

[9] Y. A. Kuznetsov, *Elements of applied bifurcation theory*, vol. 122 of Applied Mathematical Sciences, Springer-Verlag, New York, third ed, 2004.

[10] J. Llibre and C. Valls, *Global phase portraits of quadratic systems with a complex ellipse as invariant algebraic curve*, Acta Math. Sin. (Engl. Ser.), 34 (2018), pp. 801-811.

[11] L. Markus, *Global structure of ordinary differential equations in the plane*, Trans. Amer. Math. Soc, 76 (1954), pp. 127-148.

[12] D. A. Neumann, *Classification of continuous flows on 2-manifolds*, Proc. Amer. Math. Soc, 48 (1975), pp 73-81.

[13] M. M. Peixoto, *Structural stability on two-dimensional manifolds*, Topology, 1 (1962), pp. 101-120.

[14] M. M. Peixoto, *On the classification of flows on 2-manifolds*, in Dynamical systems (Proc. Sympos, Univ. Bahia, Salvador, 1971), 1973, pp. 389-419.

[15] W. F. Pereira and C. Pessoa, *A class of reversible quadratic polynomial vector fields on* $\mathbb{S}^2$, J. Math. Anal. Appl, 371 (2010), pp. 203-209.

[16] W. F. Pereira and C. Pessoa, *On the reversible quadratic polynomial vector fields on* $\mathbb{S}^2$, J. Math. Anal. Appl, 396 (2012), pp. 455-465.

[17] L. M. Perko, *Differential equations and dynamical systems*, vol. 7 of Texts in Applied Mathematics, Springer-Verlag, New York, third ed, 2001.

[18] L. M. Perko, *Global families of limit cycles of planar analytic systems*, Trans. Amer. Math. Soc, 322 (1990), pp. 627-656.

[19] L. M. Perko, *Homoclinic loop and multiple limit cycle bifurcation surfaces*, Trans. Amer. Math. Soc, 344 (1994), pp. 101-130.

[20] J. Sotomayor, *Generic one-parameter families of vector fields on two-dimensional manifolds*, Inst. Hautes Éstudes Sci. Publ. Math, (1974), pp. 5-46.
[21] J. Sotomayor, *Curvas Definidas por Equações Diferenciais no Plano*, IMPA, 1981, 13ºColóquio Brasileiro de Matemática.
[22] M. A. Teixeira, *Singularities of reversible vector fields*, Phys. D, 100 (1997), pp. 101-118.
[23] Y. Tian and Y. Zhao, *Global phase portraits and bifurcation diagrams for Hamiltonian systems of linear plus quartic homogeneous polynomials symmetric with respect to the y-axis*, Nonlinear Anal, 192 (2020), pp. 111658, 27.

[1] IBILCE–UNESP, CEP 15054–000, S. J. Rio Preto, São Paulo, Brazil

Email address: claudio.buzzi@unesp.br

[2] Universitat Autònoma de Barcelona, 08193 Bellaterra, Barcelona, Spain

Email address: jllibre@mat.uab.cat

[3] IBILCE–UNESP, CEP 15054–000, S. J. Rio Preto, São Paulo, Brazil

Email address: paulo.santana@unesp.br